

# Efficient Acid-Catalyzed Conversion of Phenylglyoxal to Mandelates on Flame-Derived Silica/Alumina

Zichun Wang,<sup>†</sup> Yijiao Jiang,<sup>‡,§</sup> Alfons Baiker,<sup>\*,‡,⊥</sup> and Jun Huang<sup>\*,†</sup>

<sup>†</sup>Laboratory for Catalysis Engineering, School of Chemical and Molecular Engineering, The University of Sydney, Sydney, New South Wales 2006, Australia

<sup>‡</sup>Institute for Chemical and Bioengineering, Department of Chemistry and Applied Biosciences, ETH Zürich, HCI, CH-8093 Zürich, Switzerland

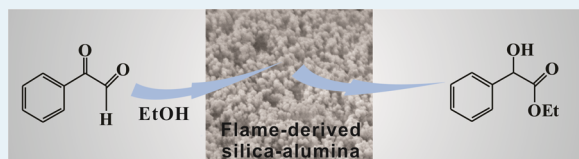
<sup>§</sup>School of Chemical Engineering, The University of New South Wales, Sydney, New South Wales 2052, Australia

<sup>⊥</sup>Chemistry Department, Faculty of Science, King Abdulaziz University, P.O. Box 80203, Jeddah 21589, Saudi Arabia

## Supporting Information

**ABSTRACT:** Amorphous, nonporous silica/alumina (SA) made by flame-spray pyrolysis (FSP) efficiently catalyzes the direct conversion of phenylglyoxal (PG) to alkyl mandelates. The SAs exhibited a turnover frequency more than an order of magnitude higher than dealuminated zeolite Y, which hitherto has been considered as the most active solid acid for this reaction. The free diffusion of PG to surface acid sites and rapid removal of mandelate products are proposed to be at the origin of the superior performance of SAs. The recyclability of the catalyst was tested in five repetitive runs and showed no significant loss of catalyst performance.

**KEYWORDS:** silica–alumina, Brønsted acidity, flame spray pyrolysis, phenylglyoxal, Cannizzaro reaction



The synthesis of mandelic acid and its derivatives is of great interest because of their important application as chiral building blocks in the synthesis of pharmaceuticals and fine chemicals.<sup>1,2</sup> Considerable effort has been expended to search for efficient production methods for these compounds.<sup>3–9</sup> Redox disproportionative conversion of aromatic aldehydes such as phenylglyoxal (PG) provides a single-step method for the synthesis of mandelates. For this purpose, both bases and acids were originally used according to the mechanism shown in Scheme 1. The intramolecular Cannizzaro reaction<sup>10</sup> was regarded as the key step in this reaction, which is initiated by the attack of the hydroxyl ion on PG in a base system, followed by hydrolysis in water or alcohol (alcoholysis) to yield mandelic acid or mandelates (see mechanism A, Scheme 1). However, a deficiency of this method is that strong Brønsted acids, such as H<sub>2</sub>SO<sub>4</sub>, catalyze the conversion of PG in alcohol to the corresponding acetals (see mechanism B, Scheme 1).<sup>7</sup> Later, homogeneous Lewis acids containing transition metal complexes or enzymatic catalysts were employed to produce mandelic acid and its derivatives from PG because the reaction could be carried out under milder conditions.<sup>4,5,12–14</sup> The highest selectivity (96.9%) and yield (94%) of ethyl mandelate (EM) were obtained with cobalt Schiff's base complexes at 333 K in 8 h; however, inherent disadvantages of these processes arise from the need of large amounts of catalyst and their toxic and corrosive nature as well as from problems connected with catalyst separation, regeneration, and the occurrence of competitive side reactions.

Most of these deficiencies could be avoided by employing suitable solid acids,<sup>15–17</sup> which have attracted great attention as alternative catalysts for the production of mandelates.<sup>11</sup> Recently, several zeolites and metal (Al, Ga, Sn and Ti)-doped MCM-41 have been tested for the catalytic conversion of trioses to  $\alpha$ -hydroxyl carboxylates in alcohols,<sup>11,18–20</sup> including phenylglyoxal.<sup>11</sup> It was concluded that the reaction pathways on these nanoporous solid acids<sup>11,18–20</sup> are similar to the intramolecular Cannizzaro reaction between the  $\alpha$ -keto aldehyde and alcohols in homogeneous catalytic systems.<sup>4,5,14</sup> Considering the catalytic conversion of PG in ethanol, both high yield (95%) and selectivity (97%) to ethyl mandelate (EM) were achieved by dealuminated USY zeolites (Si/Al = 2.6, 27% framework Al).<sup>11</sup>

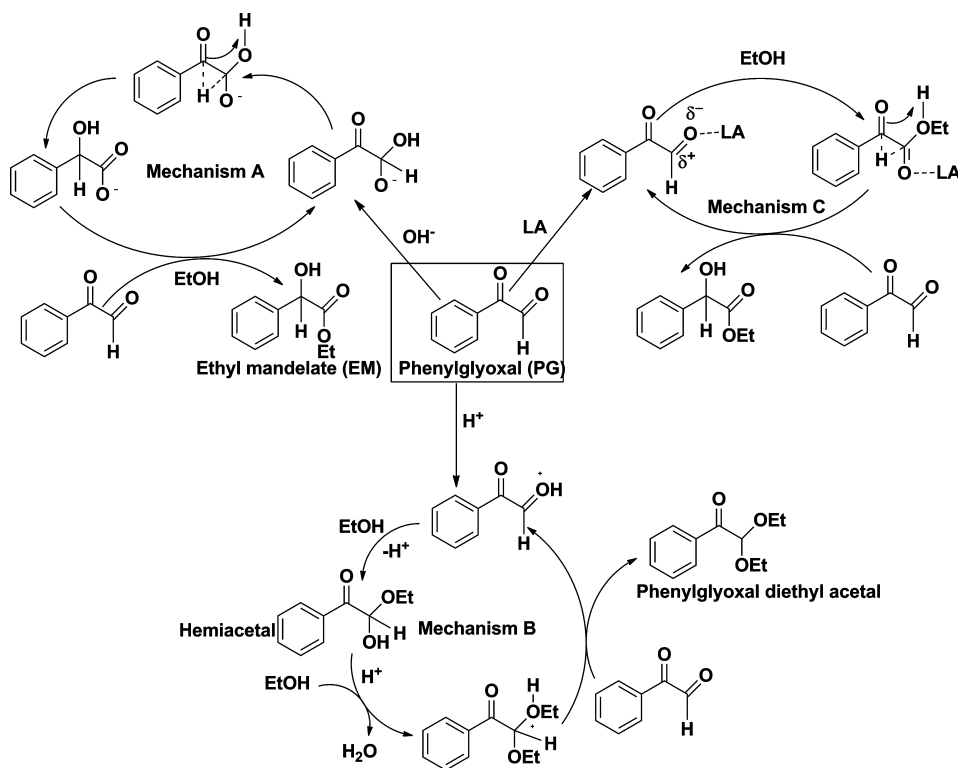
Recently, we developed unique nonporous amorphous silica–alumina (SA) catalysts with a wide range of acidity by flame-spray pyrolysis.<sup>21</sup> The SAs were synthesized in microseconds at extremely high temperature ( $\sim 2000$  K). Unlike zeolites or other porous catalysts, these thermally stable nonporous nanoparticles do not exhibit any shape or size limitation for reactant/product diffusion to surface acid sites, rendering them particularly interesting for the conversion of bigger reactant molecules and intramolecular reactions. Here, we investigated the efficiency of SAs with various Si/Al ratios in

Received: April 11, 2013

Revised: May 31, 2013

Published: June 5, 2013

Scheme 1. Proposed Reaction Mechanisms of Catalytic Conversion of PG in EtOH: (A) Pathway in Homogeneous Base System;<sup>8,10</sup> (B) Pathway in Homogeneous Brønsted Acid System;<sup>7</sup> (C) Pathway on Lewis Acid Sites<sup>5,11</sup>



the catalytic conversion of PG in ethanol and other alkyl alcohols to the corresponding mandelates.

The flame-made silica/alumina powders are designated as SA/*X*, where *X* is 0, 10, 30, 50, and 70 and indicates the mole percentage of Al in the Si/Al mixed oxide. SEM investigations (Figure 1) indicated that most of the amorphous SA catalysts showed spherical morphology with particle sizes of 7–20 nm.

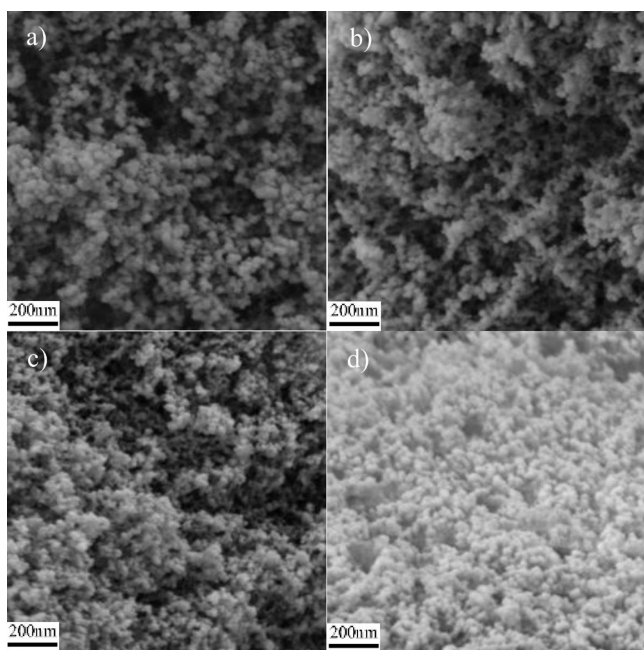


Figure 1. SEM images of (a) SA/10, (b) SA/30, (c) SA/50, and (d) SA/70.

Nitrogen adsorption/desorption isotherms of SAs (Figure S1 in the Supporting Information) indicated the typical characteristics of dispersed nonporous particles. Table 1 summarizes the BET surface areas and the results from acidity characterization of SAs and a reference catalyst De-Al-HY. The surface area of SAs decreases with higher aluminum content as a result of the incorporation of Al into the silica network, affording the formation of Brønsted acidity in SAs. The high BET surface area of zeolite De-Al-HY (particle size range 200–300 nm)

Table 1. Catalytic Data of PG Conversion to Ethyl Mandelate over SAs and De-Al-HY

catalyst	$A_{\text{BET}}^a$ $\text{m}^2/\text{g}$	$Y_{\text{EM}}^b$ (%)	$S_{\text{EM}}^c$ (%)	$\text{BA}^d$ mmol/g	$\text{LA}^e$ mmol/g	$\text{TOFs}^f$ ( $\text{h}^{-1}$ )
SA/0	156	0	0	0	0	0
SA/10	377	56	93	0.098	0	10.2
SA/30	248	67	94	0.111	0	10.5
SA/50	222	81	95	0.134	0.003	10.5
SA/70	200	97	97	0.151	0.008	10.5
De-Al-HY <sup>22</sup>	671	81	90	0.865	1.75	0.57

<sup>a</sup>The surface areas ( $A_{\text{BET}}$ ) of SAs were taken from ref 8. <sup>b</sup> $Y_{\text{EM}}$  = yield of ethyl mandelate in mol %. <sup>c</sup> $S_{\text{EM}}$  = selectivity to ethyl mandelate at 50% conversion. <sup>d</sup>BA is the number of Brønsted acid sites. The BA of SAs was taken from ref 8. The BA of De-Al-HY was determined by the BA in supercages. <sup>e</sup>LA is the number of Lewis acid sites determined by <sup>13</sup>C MAS NMR spectra in ref 8 for SAs. The peak shown at ~240 ppm is assigned to acetone-<sup>13</sup>C adsorbed on Lewis acid sites. To compare the area of acetone-<sup>13</sup>C adsorbed on Lewis and Brønsted acid sites, the concentration of Lewis sites can be obtained on the basis of the concentration of the Brønsted acid sites. For De-Al-HY, the number of LA is taken from ref 9. <sup>f</sup>Average TOFs were calculated on the basis of the conversion after 6 h of reaction, including both Brønsted and Lewis acid sites.

results mainly from its internal pore structure (internal surface area), whereas the surface area of the nonporous SA particles originates exclusively from the outer accessible surface.

Quantitative  $^1\text{H}$  MAS NMR investigations with the adsorption of ammonia was used to determine the surface Brønsted acid sites on dehydrated SAs. The adsorption of acetone- $^{13}\text{C}$  has been used to distinguish Brønsted and Lewis acid sites by  $^{13}\text{C}$  MAS NMR, and the relative intensity of Lewis sites to Brønsted sites was applied to determine the number of Lewis sites. Comparison of the amount of Brønsted and Lewis acid sites of the SAs (Table 1, column 5 and 6) indicates that all SAs are mainly populated with Brønsted acid sites. Hardly any Lewis acid sites could be detected by  $^{13}\text{C}$  MAS NMR spectroscopy<sup>21</sup> at an Al content lower than 30%. In contrast, De-Al-HY contains a 2-times-higher amount of Lewis acid sites compared with Brønsted acid sites and exposes a higher number of both Brønsted and Lewis acid sites than the SA catalysts.

The catalytic reactions were carried out using a PG (0.4 M) ethanol solution at 363 K over 0.05 g of catalyst in a stirred batch reactor. The results obtained with SAs possessing different surface area and population density of Brønsted and Lewis acid sites are summarized in Table 1. Conversions of PG and selectivities to ethyl mandelate (EM) as a function of reaction time with SA/10, 30, 50, and 70 are shown in Figure 2.

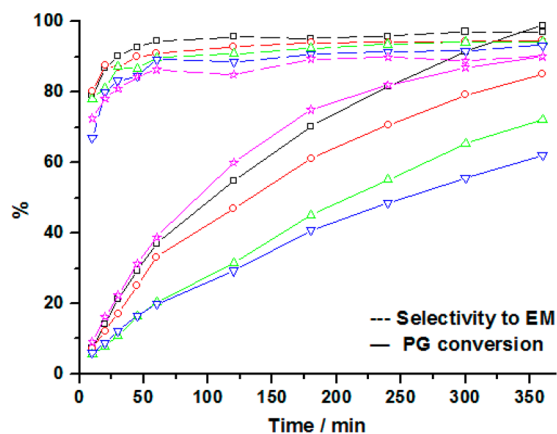


**Figure 2.** Catalytic conversion of PG in ethanol (—) and selectivity to ethyl mandelate (---) over SA/70 (□), SA/50 (○), SA/30 (△), SA/10 (▽), and De-Al-HY (☆) as a function of time. Conditions: 1.25 mL of ethanol solution containing 0.4 M PG, 0.05 g catalyst, at 363 K for 6 h with stirring.

The nonacidic SA/0 was inactive for the target reaction. After introduction of aluminum into the silica matrix, by adding Al to the precursor feed solution of the flame reactor, acidic sites were formed on the surface of the SAs<sup>21</sup> (Table 1). With increasing aluminum content, the population density of acidic sites increased, resulting in strikingly higher conversion and slightly higher selectivity to the target compound ethyl mandelate (Figure 2). The conversion of PG on different SAs after 6 h was 60% for SA/10, 71% for SA/30, 85% for SA/50, and 100% for SA/70. The increase in PG conversion correlates well with the increasing population density of acid sites on the surface of the SAs.

For comparison, the PG reaction was also performed with dealuminated zeolite H-Y (De-Al-HY) containing a large number of Lewis acid sites (1.75 mmol/g, 219 times higher than SA/70) and Brønsted acid sites (0.865 mmol/g, 6 times

higher than SA/70). PG conversion with this reference catalyst was 90% after 6 h of reaction, compared with 100% on SA/70. A comparison of the average turnover frequencies (TOFs) confirms the high activity of the SAs for PG conversion (Table 1). The average TOFs of the flame-derived SAs after 6 h were between 10.2 and 10.5  $\text{h}^{-1}$ , which is  $\sim 20$  times higher than that determined for De-Al-HY (0.57  $\text{h}^{-1}$ ). Note that De-Al-HY has much stronger acid sites (both strength and population density) and a 2–3 times higher surface area (671  $\text{m}^2/\text{g}$ , Table 1, column 2) compared with SA/10 and SA/30 (377 and 248  $\text{m}^2/\text{g}$ , respectively).<sup>21,22</sup> Striking differences between the SAs and De-Al-HY are the strength of the acid sites and their location (accessibility). The acid sites of De-Al-HY are located inside the nanopores, whereas the SAs are virtually nonporous, and constraints imposed by intraparticle diffusion phenomena can be ruled out. On the large pore ( $\sim 1.1$  nm) zeolite De-Al-HY, PG ( $\sim 0.67$  nm) can enter into the cages; however, the rate of this size-confined diffusion of PG inside micropores is expected to be considerably lower than that of the interparticle free diffusion of PG to the surface acid sites on SAs. The slow reactant and product diffusion inside the pores of De-Al-HY obviously slows down the overall reaction rate, and consequently, the higher population density of acid sites on this catalyst does not lead to enhanced PG conversion. This scenario is further supported when comparing the reaction kinetics observed with De-Al-HY and SA/70 shown in Figure 2. At the beginning of the reaction, De-Al-HY with 16.5 times more acid sites and 3.5 times higher surface area showed only slightly higher conversion than SA/70. With the progress of the reaction, the conversion on SA/70 became higher compared with that on De-Al-HY. It appears that the large-size products formed inside the zeolite pores and the decrease in the reactant concentration slowed the global reaction rate on De-Al-HY as a result of intraparticle diffusional limitations.

As reported earlier,<sup>11</sup> dealuminated zeolite USY in the Lewis acidity domain (73% extra-framework Al as Lewis acid sites, 27% framework Al contribute Brønsted acid sites) showed high selectivity (97%) and high yield (95%) to ethyl mandelate. Therefore, Lewis acid sites were proposed to contribute mainly to the formation of ethyl mandelate, whereas Brønsted acid sites preferentially generated the corresponding acetals. Lewis acid sites are also dominant in De-Al-HY, which afforded ethyl mandelate with 90% selectivity and 81% yield in this work. Interestingly, SA/70 with mainly Brønsted acid sites showed higher selectivity and yield in ethyl mandelate production (97%). Even with SA/10 exposing only Brønsted acidity, PG was converted with a selectivity of 93% to ethyl mandelate. Interestingly, flame-derived pure alumina with dominant Lewis acid sites also afforded 94% selectivity and 87% yield to ethyl mandelate. Thus, ethyl mandelate is the preferred product on both Brønsted acidic and Lewis acidic flame-derived SAs, and increasing the strength of acid sites<sup>21</sup> has only little influence on the product selectivity.

Results of the catalytic test carried out with different alcohols as reactants over the best-performing catalyst SA/70 are summarized in Figure 3 and Table 2. Figure 3 shows how the conversion and the selectivity to the corresponding alkyl mandelates (AM) developed with reaction time. Conversion of PG varied significantly among the alkyl alcohols used, being lowest for MeOH and higher with longer alkyl chains. The selectivity to alkyl mandelates was high for all alcohols, except for *n*-butyl alcohol (87%), and much less dependent on the alkyl chain length of the alcohol. The reference catalyst De-Al-

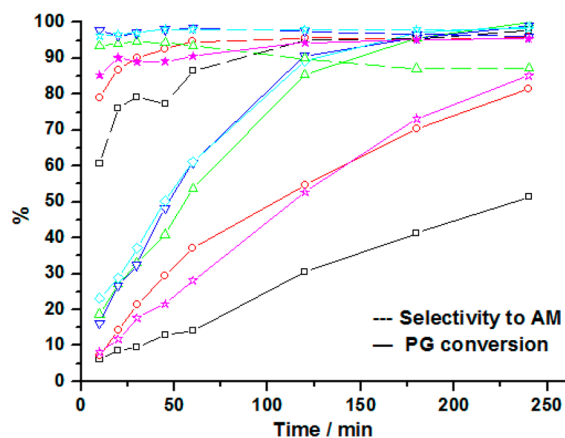


**Figure 3.** PG reaction over SA/70 in different alkyl alcohols: MeOH ( $\square$ ), EtOH ( $\circ$ ), *i*-PrOH ( $\nabla$ ), *n*-PrOH ( $\diamond$ ), *n*-BuOH ( $\triangle$ ). Catalytic conversion of PG (—) and selectivity to alkyl mandelate (---) as a function of reaction time. Reaction in isopropyl alcohol, *i*-PrOH ( $\star$ ), was carried out over De-Al-HY at the same conditions. Conditions: 1.25 mL of alcohol solution containing 0.4 M PG, 0.05 g SA/70 catalyst, at 363 K for 4 h with stirring.

**Table 2. Catalytic Results of PG Conversion in Different Alcohols to Corresponding Alkyl Mandelate over SA/70<sup>a</sup>**

ROH	$C_{\text{phenylglyoxal}}$ (%)	$Y_{\text{mandelate}}$ (%)	$S_{\text{mandelate}}$ (%)
MeOH	51	50	98
EtOH	82	78	96
<i>n</i> -PrOH	99	97	98
<i>n</i> -BuOH	100	87	87
<i>i</i> -PrOH	99	95	96
<i>i</i> -PrOH <sup>b</sup>	85	81	95

<sup>a</sup>Conditions: 1.25 mL of alcohol solution containing 0.4 M PG, 0.05 g SA/70 catalyst, at 363 K for 4 h with stirring. <sup>b</sup>PG in *i*-PrOH catalyzed by De-Al-HY at the above conditions.

HY showed considerably lower PG conversion (85 vs 99%) than SA/70 at about similar selectivity in isopropyl alcohol. As previously reported,<sup>4,5</sup> the yield to isopropyl mandelate using toxic chlorinated solvent and homogeneous catalysts ( $\text{Cu}(\text{OTf})_2$ ) was 89% and required a long reaction time (24 h) and high catalyst loading (10 mol %). Obviously, SA catalysts provide an efficient alternative and an environmentally friendly production of alkyl mandelate.

The reusability of the SAs catalysts was tested with the best-performing catalyst SA/70 in the reaction to ethyl mandelate using the standard conditions specified in Table 1. Recycling the catalyst five times did not lead to a significant change of the catalytic behavior (conversion slightly decreased from 100% to 99%, and selectivity to ethyl mandelate remained at 97%).

In conclusion, flame-made SAs offer an attractive alternative for the environmentally benign synthesis of  $\alpha$ -hydroxy esters from PG in the corresponding alcohols. High yields to ethyl mandelate (97%) and isopropyl mandelate (95%) were achieved under mild conditions in 6 and 4 h, respectively. The SAs with average TOFs of about  $10 \text{ h}^{-1}$  and up to 97% selectivity to ethyl mandelate outperformed dealuminated zeolites Y (average TOF of  $0.57 \text{ h}^{-1}$ ), which was hitherto considered as the most active solid acid for PG conversion. The high reaction rate of the flame-made SAs is attributed to their favorable nonporous structure, affording free reactant/product

diffusion to the surface acid sites. Further work about the detailed reaction mechanism is currently in progress.

## EXPERIMENTAL SECTION

SA catalysts were prepared by flame-spray pyrolysis as described elsewhere.<sup>21</sup> Dealuminated zeolite De-Al-HY ( $n_{\text{Si}}/n_{\text{Al}} = 5.4$ ) was obtained by steaming zeolite H-Y ( $n_{\text{Si}}/n_{\text{Al}} = 2.7$ ) at 748 K for 2.5 h.<sup>22</sup> Surface areas ( $A_{\text{BET}}$ ) of these catalysts were measured by  $\text{N}_2$  adsorption/desorption isotherms using the BET method at 77 K on an Autosorb IQ-C system. SEM images of all catalysts were taken on a FESEM, Zeiss Ultra+.

Catalytic studies of PG to EM conversion were performed over SAs and zeolites using the following conditions: 0.05 g catalyst was activated in a U-tube with  $\text{N}_2$  (50 mL/min) at 673 K overnight. After the catalyst cooled in  $\text{N}_2$ , 1.25 mL of alcohol solution containing 0.4 M PG was added to the glass vial with preactivated catalyst. The reaction was carried out in tightly closed glass vials in an oil bath at 363 K with stirring for 6 or 4 h. In the catalyst recycling experiments (five recycles), the used catalyst was washed with ethanol three times and dried overnight at 373 K before calcining at 773 K for 3 h for complete removal of organic residues. The reaction mixture was analyzed using a Shimadzu GCMS-QP2010 Ultra with an Rtx-SMS column (30 m  $\times$  0.25 mm  $\times$  0.25  $\mu\text{m}$ ) and quantified by a Shimadzu GC-FID equipped with a 25QC3/BP1 column (25 m  $\times$  0.32 mm  $\times$  5  $\mu\text{m}$ ). The selectivity to specific product(s)  $i$  ( $S_i$ ) was calculated as  $S_i (\%) = 100 \times [i]/([PG]_0 - [PG])$ , where  $[i]$  is the molar concentration of the product(s) and  $[PG]_0$  and  $[PG]$  correspond to the molar concentration of PG before and after reaction, respectively.

## ASSOCIATED CONTENT

### Supporting Information

Nitrogen adsorption–desorption isotherms of SAs and De-Al-HY. This material is available free of charge via the Internet at <http://pubs.acs.org>.

## AUTHOR INFORMATION

### Corresponding Author

\*E-mail: (A.B.) [baiker@chem.ethz.ch](mailto:baiker@chem.ethz.ch), (J.H.) [jun.huang@sydney.edu.au](mailto:jun.huang@sydney.edu.au).

### Notes

The authors declare no competing financial interest.

## ACKNOWLEDGMENTS

This work was supported by the Early Career Research Scheme and the Major Equipment Scheme from the University of Sydney. We also thank Niels van Vegten for help in the flame synthesis of the catalysts.

## REFERENCES

- (1) Coppola, G. M.; Schuster, H. F.,  *$\alpha$ -Hydroxy Acids in Enantioselective Synthesis*; VCH, Weinheim: Germany, 1997.
- (2) Corma, A.; Iborra, S.; Velty, A. *Chem. Rev.* **2007**, *107* (6), 2411–2502.
- (3) Abaee, M. S.; Sharifi, R.; Mojtahedi, M. M. *Org. Lett.* **2005**, *7* (26), 5893–5895.
- (4) Ishihara, K.; Yano, T.; Fushimi, M. *J. Fluorine Chem.* **2008**, *129* (10), 994–997.
- (5) Russell, A. E.; Miller, S. P.; Morken, J. P. *J. Org. Chem.* **2000**, *65* (24), 8381–8383.
- (6) Ayres, E. B.; Hauser, C. R. *J. Am. Chem. Soc.* **1943**, *65*, 1095–1096.

- (7) Manning, D. T.; Stansbury, H. A. *J. Am. Chem. Soc.* **1959**, *81* (18), 4885–4890.
- (8) Doering, W. V.; Taylor, T. I.; Schoenewaldt, E. F. *J. Am. Chem. Soc.* **1948**, *70* (2), 455–457.
- (9) Curini, M.; Epifano, F.; Genovese, S.; Marcotullio, M. C.; Rosati, O. *Org. Lett.* **2005**, *7* (7), 1331–1333.
- (10) Alexander, E. R. *J. Am. Chem. Soc.* **1947**, *69* (2), 289–294.
- (11) Pescarmona, P. P.; Janssen, K. P. F.; Delaet, C.; Stroobants, C.; Houthoofd, K.; Philippaerts, A.; De Jonghe, C.; Paul, J. S.; Jacobs, P. A.; Sels, B. F. *Green Chem.* **2010**, *12* (6), 1083–1089.
- (12) Hall, S. S.; Doneyko, A. M.; Jordan, J. *J. Am. Chem. Soc.* **1976**, *98* (23), 7460–7461.
- (13) Hall, S. S.; Doneyko, A. M.; Jordan, F. *J. Am. Chem. Soc.* **1978**, *100* (18), 5934–5939.
- (14) Maruyama, K.; Murakami, Y.; Yoda, K.; Mashino, T.; Nishinaga, A. *J. Chem. Soc., Chem. Commun.* **1992**, No. 21, 1617–1618.
- (15) Busca, G. *Chem. Rev.* **2007**, *107* (11), 5366–5410.
- (16) Corma, A. *Chem. Rev.* **1995**, *95* (3), 559–614.
- (17) Chai, S. H.; Wang, H. P.; Liang, Y.; Xu, B. Q. *Green Chem.* **2008**, *10* (10), 1087–1093.
- (18) de Clippel, F.; Dusselier, M.; Van Rompaey, R.; Vanelderden, P.; Dijkmans, J.; Makshina, E.; Giebeler, L.; Oswald, S.; Baron, G. V.; Denayer, J. F. M.; Pescarmona, P. P.; Jacobs, P. A.; Sels, B. F. *J. Am. Chem. Soc.* **2012**, *134* (24), 10089–10101.
- (19) Li, L.; Stroobants, C.; Lin, K. F.; Jacobs, P. A.; Sels, B. F.; Pescarmona, P. P. *Green Chem.* **2011**, *13* (5), 1175–1181.
- (20) Lin, K. F.; Li, L.; Sels, B. F.; Jacobs, P. A.; Pescarmona, P. P. *Catal. Today* **2011**, *173* (1), 89–94.
- (21) Huang, J.; van Vegten, N.; Jiang, Y.; Hunger, M.; Baiker, A. *Angew. Chem., Int. Ed.* **2010**, *49* (42), 7776–7781.
- (22) Huang, J.; Jiang, Y. J.; Marthala, V. R. R.; Ooi, Y. S.; Hunger, M. *ChemPhysChem* **2008**, *9* (8), 1107–1109.